



The 7th World Congress on Particle Technology (WCPT7)

## Particle agglomeration and dispersion in fully-coupled turbulent channel flow using large eddy simulation and discrete element method

Mohammed Afkhami\*, Ali Hassanpour, Michael Fairweather, Derrick O. Njobuenwu

*Institute of Particle Science and Engineering, School of Process, Environmental and Materials Engineering, University of Leeds, Leeds LS2 9JT, UK*

---

### Abstract

The work described in this paper employs large eddy simulation and the discrete element method to study particle-laden flows, including particle dispersion and agglomeration, in a horizontal channel. The particle-particle interaction model used is based on the Hertz-Mindlin approach with Johnson-Kendall-Roberts cohesion to allow the simulation of Van der Waals forces in the dry air flow considered. The influence of different particle surface energies, particle size, particle concentration and flow Reynolds numbers on particle agglomeration is investigated. The turbulent structure of the flow is found to dominate the motion of the particles, although the agglomeration rate is found to be strongly influenced by all of the variables noted above, with most of the particle-particle interactions taking place at locations close to the channel walls, aided by the higher turbulence levels and concentration of particles in these regions.

© 2015 The Authors. Published by Elsevier Ltd. This is an open access article under the CC BY-NC-ND license (<http://creativecommons.org/licenses/by-nc-nd/4.0/>).

Selection and peer-review under responsibility of Chinese Society of Particuology, Institute of Process Engineering, Chinese Academy of Sciences (CAS)

*Keywords:* Large eddy simulation; discrete element method; particles; agglomeration; channel flow.

---

---

\* Corresponding author. Tel.: +44-113-343-2351; fax: +44-113-343-2384  
*E-mail address:* [m.afkhami5@leeds.ac.uk](mailto:m.afkhami5@leeds.ac.uk)

## 1. Introduction

Particle agglomeration, dispersion and deposition processes are of relevance to a wide range of industrial applications that involve particle-laden flows in the fine chemical, pharmaceutical, and oil and gas industries, and waste management sectors, as well as being of relevance generally in aerodynamic dispersion applications, for example, in the dry powder inhalers (DPIs) used for drug delivery through the lungs. In the latter application, all of the mechanisms noted are prevalent, and critical to the functionality of the delivery process [1-4]. The dry powder in the dosing chamber of a DPI device needs to be de-agglomerated into an aerosol using the vacuum generated by a patient's inhalation. One difficulty associated with these delivery systems is in determining the deposition site of the administered dose [5]. Factors that influence deposition within the respiratory tract are the physical and chemical properties of the fluid medium and the nature of the aerosol particles. To achieve effective delivery for dry powder inhalers, the dispersion and deposition behaviour of particles in turbulent air needs to be studied to quantify the conditions favouring de-agglomeration of powders and their delivery by deposition into the lungs' airways [6].

In this work, an advanced predictive technique for describing fluid motion, namely large eddy simulation (LES), is coupled with the discrete element method (DEM) to provide further understanding of flows containing solid particles. These methods are applied to study the behaviour of single particles and how they relate to bulk behaviour, including particle dispersion, deposition and agglomeration, in a horizontal channel. The influences of different particle sizes, surface energies, concentrations and fluid flow Reynolds number are investigated.

In the context of two- and multiphase turbulent bounded flows, the most recent studies using one- and two-way coupled approaches for dispersed particle regimes mainly focus on the influence of flow structures on particle motion, and the study of non-spherical particle shapes. A recent study on one-way coupled flow by Njobuenwu and Fairweather [7], which considered the effect of particle shape on inertial particle dynamics in a channel flow, used large eddy simulation coupled to a Lagrangian particle tracking (LPT) technique. Their results showed a clear distinction between the behaviour of the various particles types, indicating the significance of particle shape when modelling many practically relevant flows. Recent work on four-way coupled flows, as considered herein, includes that of Alletto and Breuer [8] who used LES to predict a particle-laden turbulent flow at high mass loading downstream of a confined bluff body. The influence of fluid-particle interactions (two-way coupling) and particle-particle collisions (four-way coupling) were investigated in detail. Lain [9] described a three-dimensional Eulerian-Lagrangian calculation of confined horizontal gas-particle flows emphasising the importance of elementary processes, such as particle collisions with rough walls and inter-particle collisions, on the predicted two-phase flow variables and pressure drop along a duct. de Souza et al [10] adopted an LES-LPT approach with the goal of better understanding the interactions between particles and fluid in a vertical conical diffuser. The authors showed that, even at moderate mass loadings, particles can significantly affect the diffuser flow pattern, and reattach the otherwise separated flow under some conditions. Mallouppas and van Wachem [11] similarly used LES to simulate the behaviour of interacting particles in a turbulent channel flow. The importance of individual physical phenomena occurring in particle-laden flows was investigated through a series of simulations that were fully four-way coupled. The simulation results demonstrated that rough walls and inter-particle collisions have an important effect in redistributing particles across the channel, even for very dilute flows. Vincent et al. [12] utilised a direct numerical simulation (DNS) together with a Lagrangian volume of fluid (VOF) method to study particle flows in a vertical pipe. The authors developed a specific Eulerian volume of fluid method with Lagrangian tracking of the phase function and presented a strategy for handling particle collisions and lubrication effects. The numerical solutions were compared to existing theoretical and experimental results with good agreement found. It is worthy of note that DNS continues to be used to study such flows, although this is generally for low Reynolds number cases. Therefore one of the main challenges for LES is to compute flows with high precision at sufficiently high Reynolds numbers to more closely replicate those conditions found in practical applications.

All of this work has highlighted the importance of inter-particle collisions and their effects on fluid and particle characteristics. However, none has considered in detail the conditions that favour the agglomeration of particles. The dynamics of particle-laden fluid flows include a number of important aspects that dictate whether particle agglomeration will occur, affecting in turn particle dispersion and deposition. These include factors such as the instantaneous particle velocity, and the size, concentration, collision frequency and surface properties of the particles. As a result, many complications arise when analysing the underlying mechanisms responsible for

agglomeration. The coupling of LES and DEM is an effective approach that is capable of providing insight into these mechanisms as well as a predictive method applicable to many practically-relevant flows. The work described builds on the previous findings of Afkhami et al. [13] which used LES and DEM to demonstrate that a high particle mass loading is not required to promote particle agglomeration in turbulent channel flows.

## 2. Numerical Approach

The LES employed used a top-hat filter as this fits naturally into a finite-volume formulation. This is then used to decompose the continuity and Navier-Stokes equations for an incompressible Newtonian fluid with constant properties into resolved and unresolved fields, bringing about terms which represent the effect of the sub-grid scale (SGS) motions on the resolved scale motions. The SGS stress model employed in this work was the dynamic model of Germano et al. [14], applied using the approximate localisation procedure of Piomelli and Liu [15]. Computations were performed using the commercial CFD code ANSYS Fluent. The code implements an implicit finite-volume incompressible flow solver using a co-located variable storage arrangement. Because of this arrangement, a procedure similar to that outlined by Rhie and Chow [16] is used to prevent checkerboarding of the pressure field. Time advancement is performed via an implicit method for all transport terms, and the overall procedure is second-order accurate in both space and time. The code is parallel and uses the message passing interface HP MPI. Further information on the mathematical model employed, and the numerical algorithm and its application, may be found in the ANSYS Fluent 13.0 theory guide.

A Lagrangian approach was used to model particle motion from the instantaneous fluid velocity field in which the particles are tracked along their trajectories through the unsteady, non-uniform flow field. All particles were assumed to be soft spheres with equal diameter and density, with particles much heavier than the fluid ( $\rho_n/\rho_f \gg 1$ ) assumed. Elghobashi and Truesdell [17] have shown that the only significant forces in such systems are the Stokes drag and buoyancy force, although buoyancy was also neglected due to the effect of gravity not being considered. The shear induced Saffman lift force was taken into account as it assumes non-trivial magnitudes in the viscous sub-layer. This work uses a modified spherical, free-stream drag for calculation of the force on the particles. All fluid parameters were taken from the fluid cell element which contained the centre of the DEM particle. This treatment is therefore only valid for particles of the same size as, or smaller than, a fluid finite-volume cell; or where the change in fluid parameters (velocity, density, viscosity, etc.) over the extent of a particle remain roughly constant. The particle-laden flow was assumed to be dilute (particle volume fraction  $\sim 10^{-5}$ ), and the method incorporated full coupling between the phases, i.e. interactions between particles were considered, and the flow and particles were two-way coupled. Particle-wall collisions were assumed to be inelastic, with the coefficient of restitution set to 0.5. Particle-particle interactions were modelled using the discrete element method incorporating the contact model of Herz-Mindlin with Johnson-Kendall-Roberts cohesion to allow the simulation of the Van der Waals forces which influence particle behaviour [18]. The approach only considered the attractive forces within the contact area, i.e. the attractive inter-particle forces are of infinite short range. The particle surface attractive force was altered by specifying the interface energy,  $\Gamma$ , with the amount of interface energy influencing the cohesion of the material. The speed of disturbance waves was approximated by Rayleigh surface wave propagation based on the physical properties of the discrete medium. The time must then be sufficiently less than the Rayleigh time-step in order to ensure realistic force transmission rates in the assembly and to prevent numerical instability [19]. The flow was described by a three-dimensional Cartesian co-ordinate system ( $x$ ,  $y$  and  $z$ ) representing the streamwise, spanwise and wall-normal directions, respectively. The boundary conditions for the momentum equations were set to no-slip at the channel walls and the instantaneous flow field was considered to be periodic along the streamwise and spanwise directions, with a constant mass flux through the channel. The shear Reynolds numbers,  $Re_\tau = hu_\tau/\nu$ , used in the simulations were 150, 300 and 590 corresponding to bulk Reynolds numbers of  $Re_b \sim 2100$ , 4200 and 8260, respectively, based on the channel half height,  $h$ . The rectangular channel considered was of dimensions  $2h \times 2\pi h \times 4\pi h$ . The length of the channel in the streamwise direction was sufficiently long to capture the streamwise-elongated, near-wall turbulence structures that exist in wall-bounded shear flows. The non-uniform Cartesian grid used one million computational nodes. The initial particle positions were distributed randomly throughout the channel, with their initial velocity set to zero and with the particles coming in-line with local flow velocities with time. Particles

were assumed to interact with turbulent eddies over a certain period of time, that being the lesser of the eddy lifetime and the transition time. Particles that moved out of the channel were re-introduced into the computational domain using periodic boundary conditions. Particle and fluid densities were set to  $\rho_p = 1000$  and  $\rho_f = 1.3 \text{ kg m}^{-3}$ , respectively, with the kinematic viscosity  $\nu = 15.7 \times 10^{-6} \text{ m}^2 \text{ s}^{-1}$ . The particle relaxation time is given by  $\tau_p = \rho_p d_p^2 / 18\rho U$ , and the non-dimensional particle response time is defined as the particle Stokes number,  $St = \tau_p^+ = \tau_p / \tau_f$ , where  $\tau_f$  is a characteristic time scale of the flow (defined as  $\tau_f = \nu / u_\tau^2$ , where the shear velocity  $u_\tau = 0.118, 0.235$  and  $0.463$  for the 150, 300 and 590 shear Reynolds number flows, respectively). For the simulations presented, the particles considered were large with a relaxation time greater than the smallest fluid time scales, therefore the influence of the unresolved fluctuating velocities in the LES on particle motion was not important [20]. The surface energy, size and total number of particles considered, with the corresponding particle relaxation times, Stokes number, and other relevant parameters, are given in Table 1.

Table 1 Particle parameters used in the simulations.

$St$	Surface Energy / $\text{J m}^{-2}$	$\tau_p$	$d_p / \mu\text{m}$	Particle Number	Volume Fraction	$Re_\tau$
216	0; 0.05; 0.5; 5	$61.2 \times 10^{-3}$	150	20,000	$2.80 \times 10^{-5}$	300
54; 216; 837	0.05; 0.5	$61.2 \times 10^{-3}$	150	20,000	$2.80 \times 10^{-5}$	150; 300; 590
216	0.05	$61.2 \times 10^{-3}$	150	5,605; 71,489	$7.84 \times 10^{-6}; 1.00 \times 10^{-4}$	300
100; 25	0.05	$28.3 \times 10^{-3}; 7.1 \times 10^{-3}$	102; 51	63,607; 508,850	$2.80 \times 10^{-5}$	300

### 3. Results and Discussion

The results generated by the LES for the fluid phase were verified using DNS predictions for the various shear Reynolds number flows considered. Overall, the LES showed good agreement with the DNS, with the mean velocities and rms of fluctuating velocity components matching those of the DNS. The particle phase behaviour was also compared with one-way coupled DNS predictions, with results again in reasonable agreement with those derived on the basis of the DNS.

Figure 1 shows results for the number of particle bonds in the channel with time. It is important to note that all particle sizes and shear Reynolds numbers used were 150  $\mu\text{m}$  and 300, unless stated otherwise. The results clearly illustrate a general increase in the number of bonds with time due to the effects of flow turbulence on the particles. From the results of Figure 1(a), the rate at which the particles form bonds increases with the particle surface energy, as would be anticipated. Agglomeration is first seen to occur at around  $t = 0.001$  s; here the particles have increased their velocity to an extent where the flow turbulence now causes particle-particle interactions. Further scrutiny of the results, for all the cases considered, shows that a linear increase in particle bond numbers then continues to about  $t = 0.1$  s, after which an increasing divergence is seen between the higher (5.0 and 0.5  $\text{J m}^{-2}$ ) and the lower (0.05  $\text{J m}^{-2}$ ) surface energy particles. For the 0.05  $\text{J m}^{-2}$  particles the rate of bond formation increases roughly linearly with time after an initial period. In the higher surface energy cases, however, the trend is exponential, indicating an ever increasing rate at which particle bonds form with time. This suggests that there is some mechanism that advantages the higher surface energy particles in the formation of agglomerates, other than the surface energy alone. In regions close to the channel centre, the particles are very dispersed and not likely to come into contact with each other. Therefore, the number of bonds formed is minimal and not significantly different for all surface energies. Towards the channel walls, however, the conditions favour particle agglomeration. In the buffer layer, the particle concentration is again low; nevertheless, the number of bonds formed is proportionally higher for particles of greater surface energy as the flow turbulence is sufficiently high to be effective in causing particle-particle collisions. Near the channel walls, high particle concentrations and low levels of flow turbulence lead to a further increase in the number of bonds formed as the particle kinetic energy is low and therefore ineffective in promoting particle separation after collision. Further analysis would be beneficial in order to quantify the relationship between the particle surface energy, the pull-off force and flow turbulence, and their impact on the formation of successful Van

der Waals bonds. The dispersing behaviour of the particles and the regions in which particle bonds are formed is, however, discussed further below. At the end of the simulation ( $t = 0.2$ s), and for the 0.05, 0.5 and 5.0  $\text{J m}^{-2}$  surface energy particles, respectively, there are 195, 654 and 810 particle bonds in the flow. The greater surface energy of the 0.5  $\text{J m}^{-2}$  particles, as compared to the 0.05  $\text{J m}^{-2}$  particles, therefore gives rise to more than three times the number of bonds. However, a further increase of one order of magnitude in the surface energy to 5.0  $\text{J m}^{-2}$  does not result in an equivalent increase. This is indicative of the surface energy value nearing a threshold; hence, any further increase does not dramatically enhance particle agglomeration. From the above analysis, it is clear that the effects of flow turbulence are dominant in creating particle bonds, and that the particle surface energy is likewise a key factor in determining Van der Waals-induced particle agglomeration in the flow.

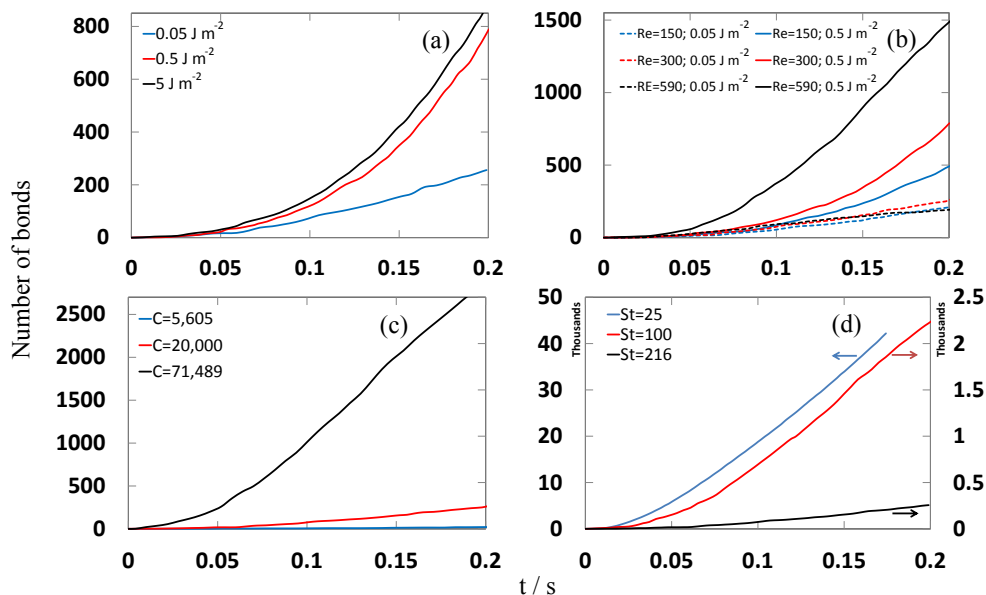


Fig. 1. Number of bonds formed between particles with time for variations in (a) particle surface energy, (b) flow Reynolds number, (c) particle concentration, and (d) particle size ( $Re_\tau=300$  except in part (b)).

The 0.05 and 0.5  $\text{J m}^{-2}$  surface energies have greater practical relevance and were therefore selected for further study. Figure 1(b) again shows the formation of particle bonds, but for three different flow Reynolds numbers. For all three shear Reynolds numbers containing 0.05  $\text{J m}^{-2}$  particles, initially the rate at which the particles form bonds increase linearly with the Reynolds number. Further scrutiny of the results shows that agglomeration first occurs at  $t \approx 0.005$ , 0.001 and 0.003 s for the  $Re_\tau = 150$ , 300 and 590 flows, respectively, indicating a slower acceleration of the particles in the  $Re_\tau = 150$  flow. The number of bonds formed in the  $Re_\tau = 590$  flow is seen to diverge from the lower Reynolds number flows and peaks at  $t \approx 0.170$  s, after which the rate of bond formation declines slightly. However, this change in the rate of bond formation is not seen for the  $Re_\tau = 150$  and 300 flows. Eventually, the bond numbers for the  $Re_\tau = 300$  and 150 flows surpass that of the  $Re_\tau = 590$  flow at  $t \approx 0.162$  and  $t \approx 0.197$  s, respectively. At the end of the simulation, and for the  $Re_\tau = 150$ , 300 and 590 flows, there are 215, 229 and 207 particle bonds, respectively. This behaviour suggests that the higher flow turbulence in the  $Re_\tau = 590$  case is responsible for creating a larger number of particle-particle interactions compared to the  $Re_\tau = 300$  and 150 flows. The subsequent decline in the rate of particle bond formation for the  $Re_\tau = 590$  case is then indicative of an increase in the rate of particle bond breakage. This behaviour can be attributed to the initial conditions; as the particles accelerate and their velocity comes in line with that of the fluid, the greater flow turbulence causes the particles to encounter more fluid resistance (due to the drag forces acting in the opposite direction to the relative motion of the particle moving with respect to the surrounding fluid), with this increased resistance responsible for the increased rate of particle bond breakage in the higher Reynolds number flow. For 0.5  $\text{J m}^{-2}$  particles, the results clearly show an increase in the

number of bonds with time; however, the rate at which the particles form bonds increases with the flow Reynolds number throughout the simulation. For all three shear Reynolds numbers, initially the rate of bond formation increases roughly linearly with time but then changes to an exponential profile. This is most apparent for the higher shear Reynolds number case. Agglomeration is first seen at approximately  $t = 0.001$  s for the 300 and 590 Reynolds number flows and at  $t = 0.01$  s in the case of the 150 Reynolds number flow. A linear increase in particle bond numbers then continues to about  $t = 0.05$  s, after which an increasing divergence is seen between the various Reynolds number flows. As for the results of Figure 1(a), this behaviour indicates a mechanism within the flow that advantages the particles exposed to higher Reynolds numbers in the formation of agglomerates. This occurs as a result of regions of high particle concentration and low particle mean velocity near the channel walls; in such regions the number of bonds formed is proportionally higher for particles of higher Reynolds number as the particles migrate to these regions at a faster rate. Moreover, the increased shear in the high Reynolds number flows increases the intensity of these turbulent regions, and therefore the particle fluctuations and hence their interactions. Further analysis is desirable to establish a quantitative relationship between the particle fluctuating velocity and its impact on the formation of successful bonds. For the  $Re_\tau = 150, 300$  and  $590$  flows, respectively, there are 528, 635 and 1524 particle bonds in the flow at the end of the simulation. These figures further reflect that increases in the flow Reynolds number dramatically enhance turbulence, and as a result particle agglomeration. It is thus again clear that the effects of turbulence are significant in creating successful particle-particle bonds, and that the flow Reynolds number is a key factor in determining particle agglomeration.

Figure 1(c) shows particle bond formation for three different particle numbers, 5,605, 20,000 and 71,489, which correspond to volume fractions of  $7.84 \times 10^{-6}$ ,  $2.80 \times 10^{-5}$  and  $1.00 \times 10^{-4}$ , respectively. A surface energy of  $0.05 \text{ J m}^{-2}$  was selected for this study. For all particle concentrations there is an increase in the number of bonds with time, with the rate at which the particle bonds form increasing with concentration. Agglomeration is first seen at approximately  $t = 0.015, 0.001$  and  $0.004$  s for the 5,605, 20,000, and 71,489 particle numbers. This reflects that for low particle concentrations the particles have to disperse a greater distance before coming into contact. For the lowest concentration flow, the rate of bond formation remains consistent and almost linear with time. In the case of the medium and high concentrations, however, initially the rate of bond formation increases roughly linearly with time but then changes to an exponential profile at about  $t = 0.02$  s, before reverting back to a linear relationship around  $t = 0.07$  s. This is most apparent for the highest concentration case, where the trend shows a more evident transition from exponential to a very steep linear relationship, indicating that the flow accelerates the particles to an approximately constant bulk particle velocity. Closer examination of the results shows that the highest concentration flow diverges from the lower concentration cases at the very start of the simulation, with the divergence increasing as the particles increase in their velocity. This trend is again repeated at  $t = 0.06$  s where the medium concentration flow deviates at an increasing rate from the low concentration case. For the low, medium and high volume fraction flows, respectively, there are 21, 265 and 2,675 particle bonds in the flow at the end of the simulation. These figures demonstrate that a three and a half fold increase in particle number dramatically increases the number of particle bonds. It is thus clear that the collision frequency in turbulent flows is not directly proportional to the particle concentration, i.e. an increase in particle number gives an exponential rise in the number of particle bonds.

Figure 1(d) shows particle bond formation for three different particle sizes;  $51 \mu\text{m}$ ,  $102 \mu\text{m}$  and  $150 \mu\text{m}$ , where for an equal volume fraction of  $2.8 \times 10^{-5}$ , there are 508,850, 63,607 and 20,000 particles in the flow, respectively. Again, a surface energy of  $0.05 \text{ J m}^{-2}$  was selected for further study. For all particle sizes, the rate of bond formation increases roughly linearly with time after an initial period. The results show an inverse relationship between particle size and the rate at which particle bonds form, indicated by the steeper gradient of the smaller particle results. Agglomeration is first seen to occur at around  $t = 0.001$  s for all particle sizes. For the  $51 \mu\text{m}$  particles, the number of bonds increases smoothly with time, whereas in the larger particle cases the trend is more variable, indicating a higher rate of bond breakage. This difference in bond breakage is explained by the differences in particle numbers, the cubed power-law relationship between particle radius and the particle overlap region, the fact that smaller particles encounter less fluid drag, and lastly larger particles having greater momentum for the collision which could lead to the breakage of the bonds. At the end of the simulation, for the  $51, 102$  and  $150 \mu\text{m}$  particles, there are 229, 2,247 and 42,209 particle bonds in the flow, respectively. Reducing the particle diameter one half from  $150$  to  $102 \mu\text{m}$ , for an equivalent volume fraction, therefore results in a 10 fold increase in bond number, with a further reduction to  $51 \mu\text{m}$  giving rise to more than 18 times the number of bonds. A further reduction in particle size may

not, however, necessarily lead to an increase in the number of particle bonds formed, as very small particles have low inertia and tend to track the fluid flow. From the above analysis, it is clear that the effects of flow turbulence are similar across all particle sizes (or Stokes numbers), and that the particle size is likewise a key factor in determining particle agglomeration in the flow. To further understand the extent to which particle size affects the mechanisms of particle agglomeration and dispersion, it is necessary to analyse in detail the particle collision frequency, the bond strength, and particle drag and dispersion, although this will be the subject of further work.

Figure 2(a-k) shows the instantaneous location of individual particles and bonds in the wall-normal direction for all cases given in Table 1, and their number at each location, at time  $t = 0.2$  s. Results are shown for 50 equally spaced regions across half the channel height, with particle statistics combined within each of the slabs of fluid considered. The columns for the number of bonds are plotted in relation to the channel walls, with column 1 adjacent to the lower and upper walls and column 50 at the channel centre. In order to compare the effects of different variables on particle agglomeration in flows with different particle concentrations, the local number of bonds,  $B=B(s)$ , has been normalised by the total number of bonds,  $B_t$ . Furthermore, the local particle concentration  $C=C(s)$ , has been normalised against the concentration,  $C_0$ , at an earlier time step of  $t = 0.1$  s so that the results are independent of the initial conditions imposed on the particles. To investigate the effects of surface energy on particle agglomeration, three particles of different surface energies were selected for a shear Reynolds number flow of 300; these include  $0.05 \text{ J m}^{-2}$  (Figure 2(f)),  $0.5 \text{ J m}^{-2}$  (Figure 2(g)) and  $5.0 \text{ J m}^{-2}$  (Figure 2(h)). The results shows that at the channel centre the number of normalised bonds is 1.61, 0.21 and 0.24, respectively, with these values increasing towards the walls, where for columns 1 and 2 they increase to an average of 3.23, 6.89 and 8.88, and 2.82, 5.03 and 4.47, respectively. Therefore, relative to the total number of particle bonds present, particle agglomeration at the channel centre is highest for the lowest surface energy particles, whereas close to the walls (column 1) agglomeration is highest for the highest surface energy particles. Further away from the walls (column 2) it is highest for the medium surface energy particles. These results indicate, therefore, that particle surface energy is important in the formation of particle-particle bonds, as might be anticipated, although less effective in resisting bond breakage due to the effects of flow turbulence. This is most likely due to flow turbulence increasing the pull-off force of the higher surface energy particles leading to their separation.

The effect of flow Reynolds number on particle agglomeration for low surface energy ( $0.05 \text{ J m}^{-2}$ ) particles is considered in the results for three  $Re_\tau$ ; 150 (Figure 2(a)), 300 (Figure 2(f)) and 590 (Figure 2(j)). The results show that for low surface energy particles, the level of turbulence in the  $Re_\tau=300$  flow is the most effective in forming particle agglomerates. In the case of the medium surface energy ( $0.5 \text{ J m}^{-2}$ ) particles, for  $Re_\tau=150$  (Figure 2(b)), 300 (Figure 2(g)) and 590 (Figure 2(k)), the particle behaviour reflects the higher turbulence levels in the 590 flow, which drives the particles to regions of lower fluid velocity. Throughout the  $Re_\tau=590$  flow, particle agglomeration is enhanced through high fluctuating velocities which affect a high number of particle-particle interactions, with peak levels approximately 30 wall units away from the solid boundaries. This effect is therefore most evident in the results for columns 2-5, which contain the highest agglomerate number, excluding those regions closest to the walls where particle concentrations are high.

The effects of particle concentration on agglomeration are investigated by comparing low surface energy particles ( $0.05 \text{ J m}^{-2}$ ) at low (5,605, Figure 2(e)), medium (20,000, Figure 2(f)), and high (71,489, Figure 2(i)) concentrations. In the low concentration flow, particles form bonds in different regions of the channel and are well dispersed, whereas a large number of particles are segregated at the walls. A higher fraction of bonds are present closer to the channel walls, with columns 1-5 containing 14.3% of the total number of bonds. The medium concentration flow contains particle-particle bonds that are more concentrated closer to the channel walls, with columns 1-5 accounting for 23.8% of the total number of bonds. Lastly, in the high concentration flow, particle bonds are again well dispersed, as seen in the lower concentration flow, where columns 1-5 contain 16.8% of the total number of bonds. This behaviour indicates that a very high concentration of particles damps the flow turbulence and/or slows down the rate of particle dispersion in the flow.

Figures 2(c), (d) and (f) compare the instantaneous distribution of particle position and bonds, but for different particle sizes (i.e. 51, 102 and  $150 \mu\text{m}$ ) and a surface energy  $0.05 \text{ J m}^{-2}$ . Again, a general increase in particle agglomeration is seen towards the channel walls. For the 51 and  $102 \mu\text{m}$  particles, at the channel centre (column 50) the normalised number of bonds is 0.43 and 0.72, with these values increasing towards the walls at a high rate,

where for columns 1 and 2 they increase to an average of 11.9 and 4.48, and 4.68 and 2.67, respectively. In contrast, the 150 μm particle bonds are more dispersed within the channel. The results therefore suggest that smaller particles have a greater propensity to form particle agglomerates throughout the channel, which is further aided by regions of high turbulence in the buffer layer and high particle concentrations at the walls.

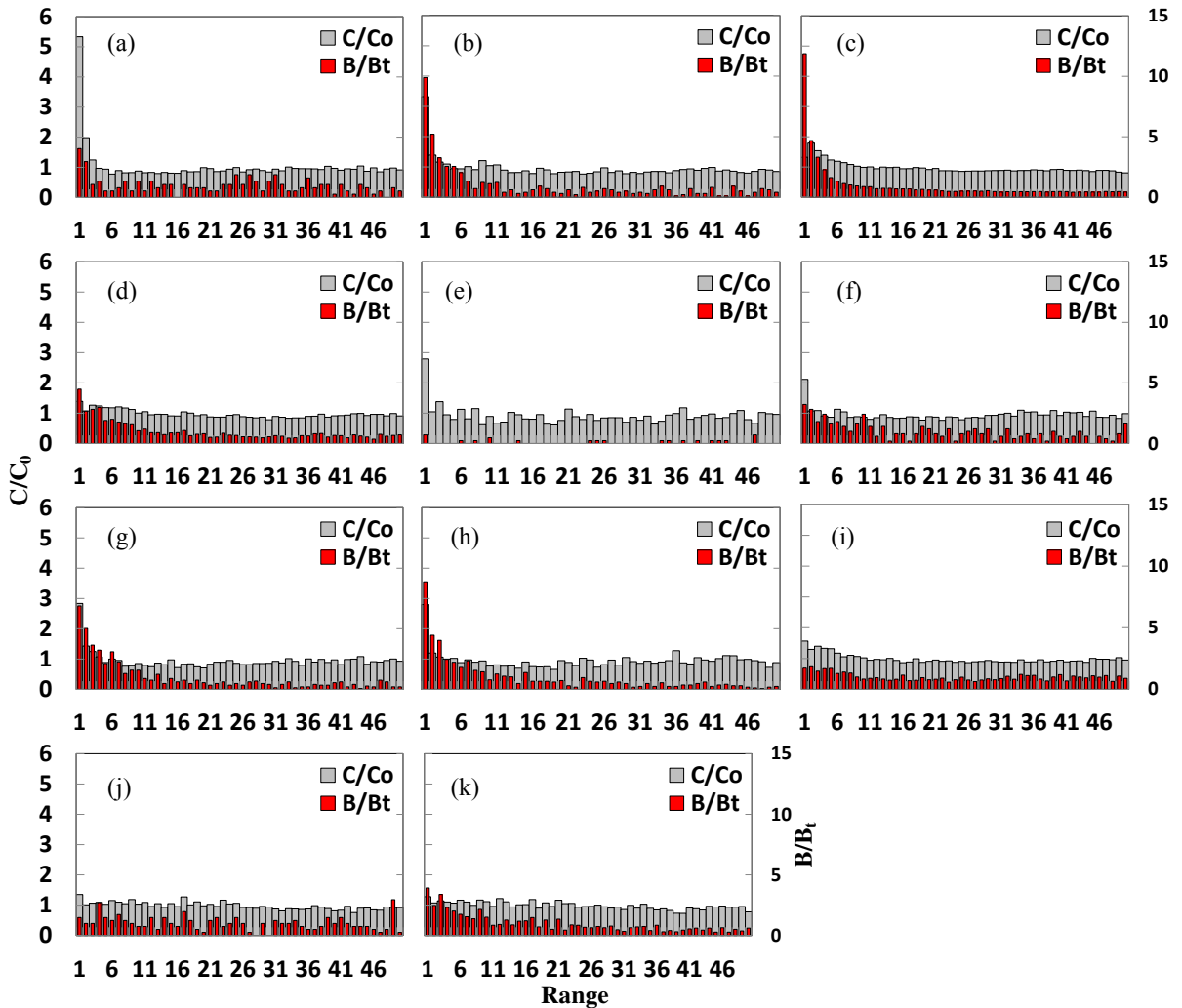


Fig. 2 Normalised bond and particle number distribution across the channel at  $t = 0.2$  s for (a)  $Re_t = 150$ ;  $150 \mu\text{m}$ ;  $0.05 \text{ J m}^{-2}$ ; 20,000 particles, (b)  $Re_t = 150$ ;  $150 \mu\text{m}$ ;  $0.5 \text{ J m}^{-2}$ ; 20,000, (c)  $Re_t = 300$ ;  $51 \mu\text{m}$ ;  $0.05 \text{ J m}^{-2}$ ; 508,850, (d)  $Re_t = 300$ ;  $102 \mu\text{m}$ ;  $0.05 \text{ J m}^{-2}$ ; 63,607, (e)  $Re_t = 300$ ;  $150 \mu\text{m}$ ;  $0.05 \text{ J m}^{-2}$ ; 5,605, (f)  $Re_t = 300$ ;  $150 \mu\text{m}$ ;  $0.05 \text{ J m}^{-2}$ ; 20,000, (g)  $Re_t = 300$ ;  $150 \mu\text{m}$ ;  $0.5 \text{ J m}^{-2}$ ; 20,000, (h)  $Re_t = 300$ ;  $150 \mu\text{m}$ ;  $5 \text{ J m}^{-2}$ ; 20,000, (i)  $Re_t = 300$ ;  $150 \mu\text{m}$ ;  $0.05 \text{ J m}^{-2}$ ; 71,489, (j)  $Re_t = 590$ ;  $150 \mu\text{m}$ ;  $0.05 \text{ J m}^{-2}$ ; 20,000, and (k)  $Re_t = 590$ ;  $150 \mu\text{m}$ ;  $0.5 \text{ J m}^{-2}$ ; 20,000.

Fig. 3(a-d) shows the time evolution of the maximum value of the particle number density near the wall. The rationale for monitoring this quantity lies in the fact that the concentration close to the wall is the one that takes longest to reach a steady state. In Figure 3(a), the results clearly show that, starting from an initial distribution corresponding to a flat profile centered around  $n_p^{\text{max}} = 1$ , the particles accumulate at the walls at an approximately linear rate. In Figure 3(b),  $n_p^{\text{max}}$  in the  $Re_t = 150, 300$  and  $590$  flows is seen to increase linearly to almost constant values at 0.23, 0.15 and 0.23 s, respectively. This behaviour suggests that the turbulence in the higher Reynolds number flows accelerates the particles at a faster rate in all directions (including towards the walls). In Figure 3(c), the higher concentration flows reach an asymptote earlier than the flow with the lowest particle concentration. This

is due to a high concentration of particles damping the flow turbulence and delaying particle drift. In Figure 3(d), two competing effects are relevant, making the analysis more complicated, namely particle concentration and Stokes number. From previous studies, however, it is known that in turbulent channel flow particle positions close to a wall correlate with instantaneous regions of low velocity along the streamwise direction, with particles avoiding regions of high velocity. The behaviour observed is consistent with previous LES and DNS results where turbophoresis is known to cause the accumulation of particles in near-wall regions, which in the present flow also enhances the rate of particle agglomeration in such regions.

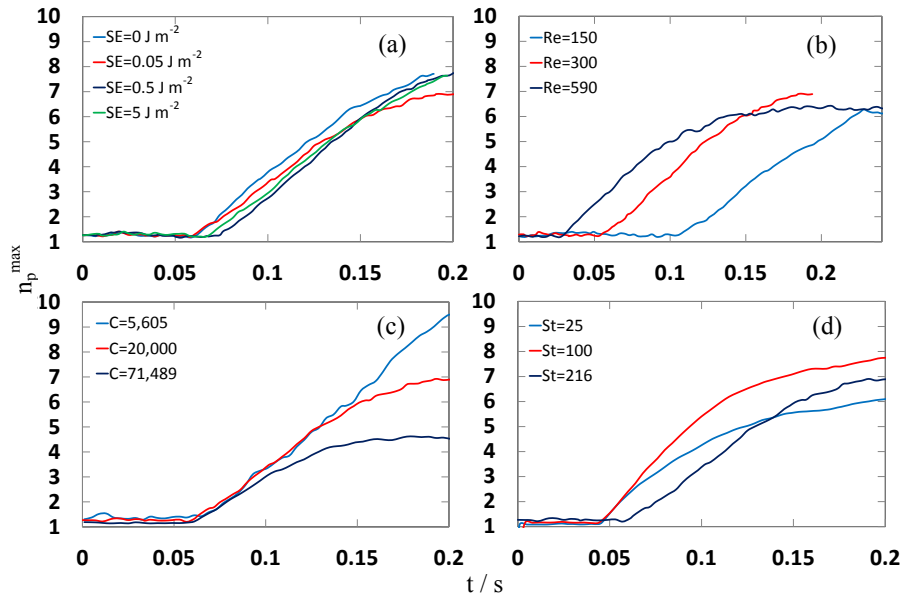


Fig. 3. Maximum value of particle number density at the wall,  $n_p^{\max}$ , as a function of time for variations in (a) surface energy, (b) Reynolds number, (c) concentration and (d) particle size ( $Re_\tau=300$  except in part (b)).

#### 4. Conclusions

The work reported has focused on the prediction of those conditions that favour particle agglomeration and dispersion within turbulent channel flows using a fully coupled LES-DEM approach. Simulations have been carried out to investigate the effects of particle size and concentration on particle agglomeration. Furthermore, particles with different surface properties have been simulated in three channel flows with different levels of flow turbulence, achieved by increasing the Reynolds number of the flow. It has been found that the turbulence structure of the flow dominates the motion of the particles, creating particle-particle interactions, with most of these interactions taking place at locations close to the channel walls and in regions of high turbulence where their agglomeration is aided both by the high levels of turbulence and the high concentration of particles. A positive relationship between particle surface energy, concentration and size, and agglomeration, was observed. Moreover, the results derived for the three Reynolds numbers considered show that the rate of agglomeration is strongly influenced for high surface energy particles by, and increases with, the intensity of the flow turbulence. In contrast, for lower surface energy particles, the rate of agglomeration diminishes with an increase in flow turbulence intensity.

#### References

- [1] J. Rosenstock, Mealtime rapid-acting inhaled insulin (Exubera<sup>®</sup>) improves glycemic control in patients with type 2 diabetes failing combination oral agents: A 3-month, randomized, comparative trial, *Diabetes* 51 (2002) 535.
- [2] T. Quattrin, A. Bélanger, N.J.V. Bohannon, S.L. Schwartz, Efficacy and safety of inhaled insulin (Exubera) compared with subcutaneous insulin therapy in patients with type 1 diabetes: Results of a 6-month, randomized, comparative trial, *Diabetes Care* 27 (2004) 2622-2627.
- [3] P.A. Hollander, L. Blonde, R. Rowe, A.E. Mehta, J.L. Milburn, K.S. Hershon, J.-L. Chiasson, S.R. Levin, Efficacy and safety of inhaled

insulin (Exubera) compared with subcutaneous insulin therapy in patients with type 2 diabetes: Results of a 6-month, randomized, comparative trial, *Diabetes Care* 27 (2004) 2356-2362.

- [4] I.M. Shaikh, K.R. Jadhav, S. Ganga, V.J. Kadam, S.S. Pisal, Advanced approaches in insulin delivery, *Current Pharmaceutical Biotechnology* 6 (2005) 387-395.
- [5] B.L. Laube, G.W. Benedict, A.S. Dobs, Time to peak insulin level, relative bioavailability, and effect of site of deposition of nebulized insulin in patients with noninsulin-dependent diabetes mellitus, *Journal of Aerosol Medicine* 11 (1998) 153-173.
- [6] K.M. Rave, L. Nosek, A. de la Peña, M. Seger, C.S. Ernest, L. Heinemann, R.P. Batycky, D.B. Muchmore, Dose response of inhaled dry-powder insulin and dose equivalence to subcutaneous insulin lispro, *Diabetes Care* 28 (2005) 2400-2405.
- [7] D. Njobuenwu, M. Fairweather, Effect of shape on inertial particle dynamics in a channel flow, *Flow, Turbulence and Combustion* 92 (2014) 83-101.
- [8] M. Alletto, M. Breuer, One-way, two-way and four-way coupled LES predictions of a particle-laden turbulent flow at high mass loading downstream of a confined bluff body, *International Journal of Multiphase Flow* 45 (2012) 70-90.
- [9] S. Laín, Pneumatic conveying of solids along a channel with different wall roughness, *Chemical Engineering Communications*, 201 (2014) 437-455.
- [10] F.J. de Souza, A.L. Silva, J. Utzig, Four-way coupled simulations of the gas-particle flow in a diffuser, *Powder Technology* 253 (2014) 496-508.
- [11] G. Mallouppas, B. van Wachem, Large eddy simulations of turbulent particle-laden channel flow, *International Journal of Multiphase Flow* 54 (2013) 65-75.
- [12] S. Vincent, J.C.B. de Motta, A. Sarthou, J.-L. Estivaleres, O. Simonin, E. Climent, A Lagrangian VOF tensorial penalty method for the DNS of resolved particle-laden flows, *Journal of Computational Physics* 256 (2014) 582-614.
- [13] M. Afkhami, A. Hassanpour, M. Fairweather, D.O. Njobuenwu, Particle-interaction effects in turbulent channel flow, in A. Kraslawski, I. Turunen (Eds.), 23<sup>rd</sup> European Symposium on Computer Aided Process Engineering, *Computer-Aided Chemical Engineering* 32, Elsevier, Amsterdam, 2013, pp. 847-852.
- [14] M. Germano, U. Piomelli, P. Moin, W.H. Cabot, A dynamic subgrid-scale eddy viscosity model, *Physics of Fluids A* 3 (1991) 1760-1765.
- [15] U. Piomelli, J. Liu, Large-eddy simulation of rotating channel flows using a localized dynamic model, *Physics of Fluids* 7 (1995) 839-848.
- [16] C. Rhie, W. Chow, Numerical study of the turbulent flow past an isolated airfoil with trailing edge separation, *AIAA J* 21 (1983) 1525-1532.
- [17] S. Elghobashi, G. Truesdell, On the two-way interaction between homogeneous turbulence and dispersed solid particles. I: Turbulence modification, *Physics of Fluids A* 5 (1993) 1790-1801.
- [18] K.L. Johnson, K. Kendall, A.D. Roberts, Surface energy and the contact of elastic solids, *Proceedings of the Royal Society of London A* 324 (1971) 301-313.
- [19] Z. Ning, M. Ghadiri, Distinct element analysis of attrition of granular solids under shear deformation, *Chemical Engineering Science* 61 (2006) 5991-6001.
- [20] J. Pozorski, S.V. Apte, Filtered particle tracking in isotropic turbulence and stochastic modeling of subgrid-scale dispersion, *International Journal of Multiphase Flow* 35 (2009) 118-128.